Research on Chemical Intermediates (2019) 45:2119–2134
https://doi.org/10.1007/s11164-018-03721-z

A three-component, one-pot synthesis of 1,8-naphthyridine and isoxazole derivatives and computational elucidation of the mechanism

Muge Guleli[1] · Safiye S. Erdem[2] · Nuket Ocal[1] · Ihsan Erden[3] · Ozlem Sari[4]

Received: 14 August 2018 / Accepted: 24 December 2018 / Published online: 9 January 2019

Abstract

An efficient and general method for the synthesis of substituted 3,4-dimethylisoxazolo[5,4-*b*]pyridine-5-carboxamide and benzo[*b*][1,8]naphthyridine-3-carboxamide derivatives by using 2,2,6-trimethyl-4H-1,3-dioxin-4-one, benzyl amine, aromatic aldehydes, 2-aminoquinoline, or 5-amino-3-methylisoxazole in the presence of a catalytic amount of *p*-toluenesulfonic acid or iodine is described. The formation of the products was investigated and the results obtained were also supported by theoretical calculations.

Keywords Isoxazoles · 1,8-Naphthyridines · Catalyst · Conjugated heterocycles · Computational studies

This paper is dedicated to Prof. Nuket Ocal. During the revision process of this manuscript, our dear colleague and friend, Prof. Nuket Ocal, tragically passed away. We are deeply grateful to Dr. Ocal's tireless efforts, dedication and her—and her students'—invaluable contributions to this project.

Electronic supplementary material The online version of this article (https://doi.org/10.1007/s11164-018-03721-z) contains supplementary material, which is available to authorized users.

✉ Safiye S. Erdem
erdem@marmara.edu.tr

✉ Nuket Ocal
nocal@yildiz.edu.tr

✉ Ihsan Erden
ierden@sfsu.edu

[1] Faculty of Arts and Sciences, Department of Chemistry, Yildiz Technical University, Davutpasa Campus, 34220 Esenler-Istanbul, Turkey

[2] Faculty of Arts and Sciences, Chemistry Department, Marmara University, 34722 Goztepe, Istanbul, Turkey

[3] Department of Chemistry and Biochemistry, San Francisco State University, 1600 Holloway Avenue, San Francisco, CA 94132, USA

[4] Department of Chemistry, Kırsehir Ahi Evran University, 40100 Kırsehir, Turkey

Introduction

Heterocyclic compounds having pharmacological, pesticidal and antimicrobial features constitute biologically active groups. The origin of important biological activities of these types of heterocyclic organic compounds can be traced to the presence of their characteristic N–C–O groups.

Nitrogen heterocycles have received a great deal of attention in the literature due to their role as active pharmacophores of historical significance. Among these heterocyclic systems, 1,8-naphthyridine derivatives are especially important because of their diverse biological activities in pharmacological and immunological systems as well as cancer treatment [1–3]. Johns and co-authors have reported oxadiazole- and triazole-substituted naphthyridines as HIV-1 integrase inhibitors. They also investigated the use of a 1,3,4-oxadiazole in combination with an 8-hydroxy-1,6-naphthyridine ring system which has been shown to deliver potent enzyme and antiviral activity through inhibition of viral DNA integration [4, 5]. Besides, isoxazoles are an important class of heterocycles that are largely employed in the area of pharmaceuticals and therapeutics such as insecticidal, antibacterial, antibiotic, antitumor, antifungal, antituberculosis, anticancer and ulcerogenic activities. Isoxazole derivatives are used in the market as COX-2 inhibitors and anti-inflammatory drugs. Isoxazole derivatives such as sulfamethoxazole, sulfisoxazole, oxacillin, cycloserine, and acivicin have been in commercial use for many years [6]. In addition, pyridine rings are associated with diverse pharmacological properties such as anticancer, antimicrobial, anticonvulsant, antiviral, anti-HlV, antifungal and antimycobacterial activities [7–9].

Moreover, C–C and C–heteroatom bond-forming reactions are very important for organic synthesis. For the reasons mentioned above, we designed a multicomponent reaction (MCR) which has the requisite features of green chemistry due to its environmental friendliness, atom economy, and minimization of waste, labor, time and cost.

This report contributes to important classes of heterocyclic compounds and provides useful synthetic methodology to access these biologically active structures. In this study, we report the successful three-component reactions of *N*-benzyl-3-oxobutanamide **3**, aromatic aldehydes and aromatic amines in the presence of a catalytic amount of *p*-toluenesulfonic acid (*p*-TsOH·H_2O) or iodine under mild reaction conditions. Because of their important structural features as well as the potential biological activities of the cyclization products, the mechanism of this reaction is also our concern. In the literature, there are a few mechanistic proposals for similar MCRs [1, 8]. To the best of our knowledge, however, there exists no computational mechanistic study for similar MCRs. Our interest here is to elucidate the mechanism of this reaction based on theoretical calculations. Recently, three-component reactions with 5-amino-3-methylisoxazole were reported by Tkachenko et al. [10] using *N*-phenyl-3-oxobutanamide in butanol without a catalyst which resulted in different positions of the aryl and methyl groups in their products with respect to our products.

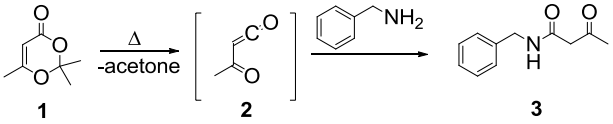

Scheme 1 Preparation of **3**

Scheme 2 Synthesis of **4a–d**

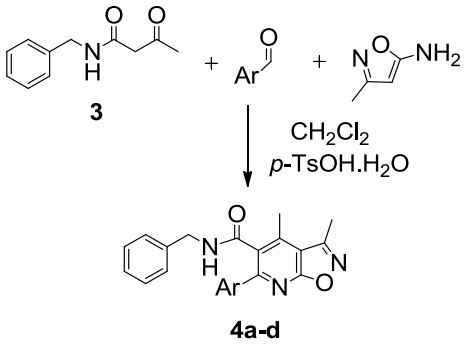

Results and discussion

Experimental results

2,2,6-Trimethyl-4H-1,3-dioxin-4-one (diketene-acetone adduct) (**1**) is an excellent acetoacetylation agent for a variety of nucleophiles, in particular for amides. It is also a useful synthetic building block for a variety of carbocycles and heterocycles. Furthermore, dioxinone **1** is a commercially available liquid which is stable at room temperature but decomposes when heated above 100 °C to give acetylketene **2** (Scheme 1) [11]. Reaction of **2** with benzylamine yields **3**.

Under the optimized conditions, the treatment of **3** with various aromatic aldehydes and 5-amino-3-methylisoxazole in the presence of catalytic *p*-TsOH.H_2O in CH_2Cl_2 gave 3,4-dimethylisoxazolo[5,4-*b*]pyridine-5-carboxamide derivatives **4a–d** in good yields (Scheme 2, Table 1).

We repeated the same reaction with 2-aminoquinoline, aromatic aldehydes and *p*-TsOH as the catalyst in dichloromethane. The spectroscopic analysis of the products validated that what we obtained were intermediate products **5a–c**, not the final-ring closure products (Scheme 3). In fact, the formation of these intermediates (**5a–c)** as well as our computational study justifies the mechanism we proposed.

Compounds **5a–c** were then refluxed with iodine at acetonitrile to obtain benzo[*b*][1,8]naphthyridine-3-carboxamides **6a–c** (Scheme 4).

The results are summarized in Table 1. Compounds **4a–d** and **5a–c** were stable solids and their structures were determined by infrared (IR), proton nuclear magnetic resonance ^{1}H NMR, and ^{13}C NMR spectroscopy and mass spectrometry (LCMSMS-QTOF). We also conducted ultraviolet (UV) studies to demonstrate that ring closure occurred in the reactions with 2-aminoquinoline (Fig. 1). The

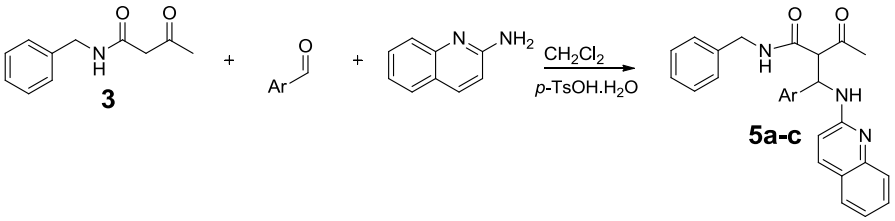

Scheme 3 Synthesis of **5a–c**

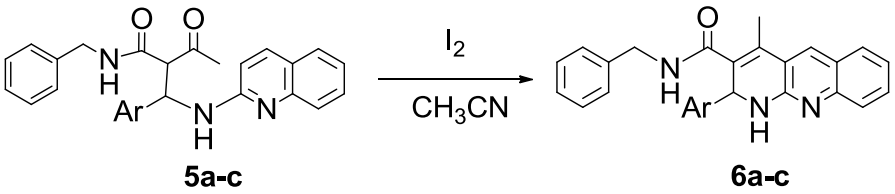

Scheme 4 Synthesis of **6a–c**

Table 1 The synthesized compounds and their yields

Entry	Ar	Product	Time (days)	Yield[a] (%)
1	4-FC_6H_4	**4a**	14	45
2	4-ClC_6H_4	**4b**	19	70
3	4-$NO_2C_6H_4$	**4c**	15	72
4	4-CNC_6H_4	**4d**	20	37
5	4-FC_6H_4	**5a**	24	42
6	4-ClC_6H_4	**5b**	20	65
7	4-CNC_6H_4	**5c**	12	47
8	4- FC_6H_4	**6a**	2	36
9	4-ClC_6H_4	**6b**	2	34
10	4-CNC_6H_4	**6c**	3	30

[a]Isolated yield

mechanism we propose for the formation of products **4a–d** and **5a–c** is illustrated in Scheme 5 using compound **4a.** This mechanism was supported by the computational study using density functional theory. Experimental evidence for the proposed mechanism stems from the formation of compounds **5a–c** under the same reaction conditions, which are the analogous intermediates **3-I3** of the 5-amino-3-methylisoxazole in Scheme 5. The reason for not observing the cyclization of **5a–c** can be attributed to the annelation effect of the fused benzene moiety in 2-aminoquinoline. Presumably, aromaticity of the benzene moiety will diminish the π-electron density of the pyridine C2–C3 bond which is required for the cyclization as shown in the **TS3-N-1** step of the mechanism in Scheme 5.

It should be noted that products **4a–d** were obtained as aromatic compounds via air oxidation. Oxygen was important for this aromatization step [12].

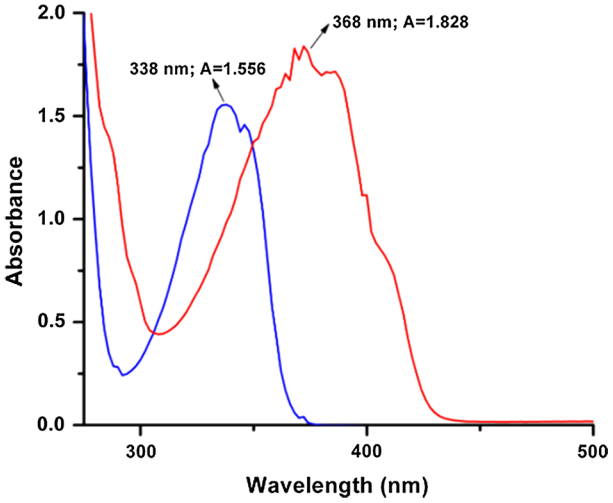

Fig. 1 UV spectra of **6a** (red) and **5a** (blue). (Color figure online)

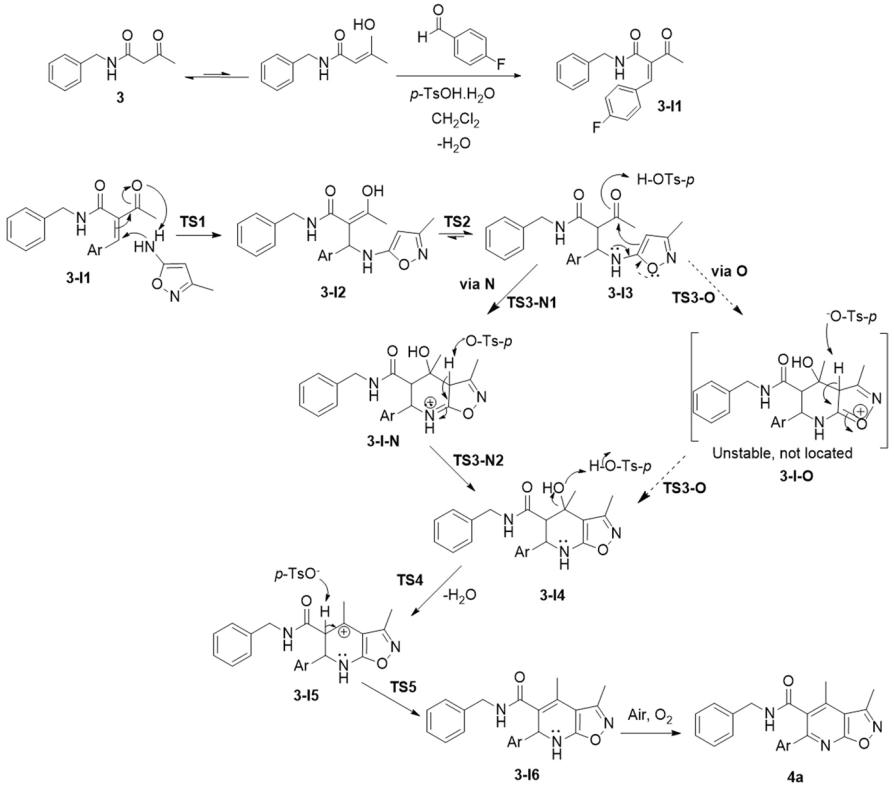

Scheme 5 The proposed mechanism for the formation of **4a**

Computational results

In the literature, several mechanistic paths are suggested for similar MCRs. Wang et al. [12] proposed the initial formation of the Schiff base followed by the addition of enol and then the intramolecular Friedel–Crafts cyclization. On the other hand, Shaabani et al. [1, 8] proposed initial condensation of *N*-alkylated-3-oxobutanamide with the aldehyde to give an intermediate analogous to **3-I1** in Scheme 5. In the next step, they postulate a Michael addition of the aromatic amine onto the vinylogous amide followed by an intramolecular condensation. Initially, we attempted to model these previous mechanistic proposals for our three-component reaction. The activation energy barrier of the Schiff base formation mechanism was calculated to be extremely high, suggesting that this mechanism is not the preferred route for our reaction (Supplementary Material, Scheme S1, Figure S47). In order to further check this mechanism, we synthesized the Schiff base and subjected it to the same reaction conditions. We did not observe the formation of the expected products. Based on this result together with the calculated high energy barrier obtained from our computational work, we excluded this mechanism. For the mechanism proposed by Shaabani et al. [1, 8], all our attempts to optimize the Michael addition intermediate were unsuccessful. Therefore, we report herein an alternative mechanism in Scheme 5 which appears to be plausible based on density functional theory calculations.

The first reaction in Scheme 5 is a well-known Knoevenagel reaction which was also proposed by Shaabani et al. [1, 8] It is expected that **3** undergoes keto-enol tautomerization. Then, the addition of enol to 4-fluorobenzaldehyde and subsequent water elimination generates intermediate **3-I1**. Since this is a well-known reaction as well, our computational studies are focused on the remaining steps (addition and cyclization of 5-amino-3-methylisoxazole) of the mechanism covering **3-I1** to **3-I6** in Scheme 5.

Calculated and relative Gibbs free energies of optimized structures are given in Table S1 (see the Supplementary Data). The Gibbs free energy profile relative to **RC1**, which is the reactant complex of intermediate **3-I1** and 5-amino-3-methylisoxazole, is given in Fig. 2. Three-dimensional (3-D) views of all the optimized structures are shown in Figs. 3 and 4. After the formation of intermediate **3-I3**, we assume two alternative paths: cyclization via the O atom of the isoxazole ring or via the N atom of the amine group. We were able to optimize the structures for the cyclization via the N path only by using the M06-2X/6-31+G(d,p) basis set. Therefore, structures related to the previous crucial steps (**TS1** and **TS2**) having relatively higher energies were also optimized with the M06-2X/6-31+G(d,p) method in order to check the energy profile. The remaining structures were optimized with the M06-2X/6-31G(d,p) method and the energy comparison of the two paths was employed by energy calculations with implicit solvent effect at the PCM/M06-2X/6-311++G(d,p) level.

In the reaction profile graph, all steps except **TS3** are common for both cyclization mechanisms. Since the inclusion of diffuse function to the basis set in the geometry-optimization process did not remarkably change the energy profile (upper profile in Fig. 2), the energetic of the common steps will be discussed based on the

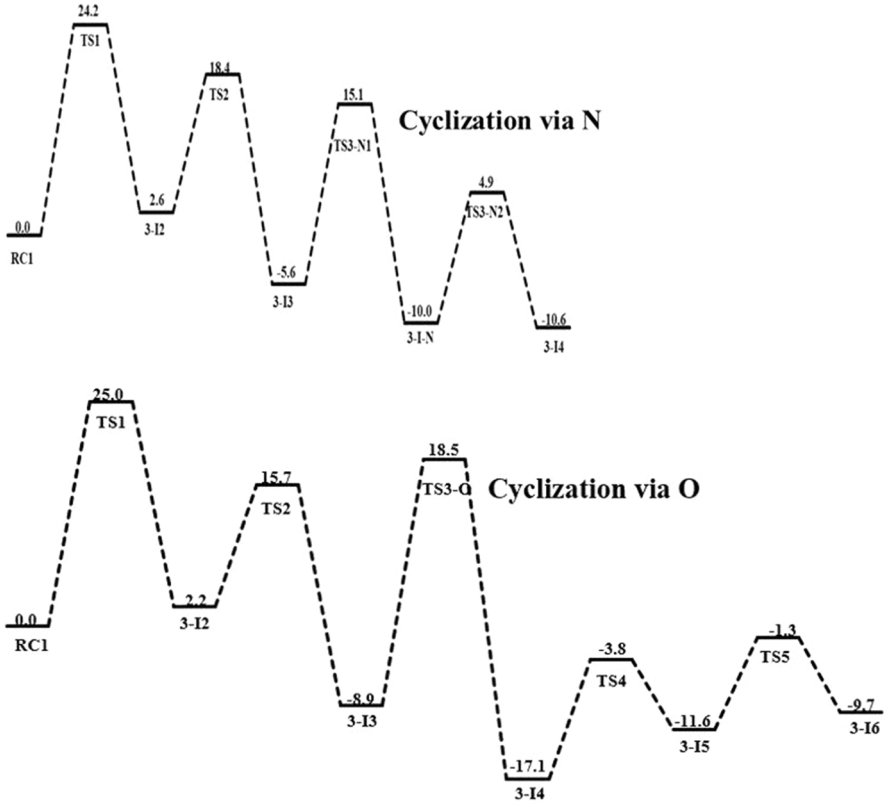

Fig. 2 Reaction profile and relative Gibbs free energies (kcal/mol) obtained from PCM/6-311++G(d,p) energies of M06-2X/6-31G(d,p) optimizations (lower profile) and M06-2X/6-31+G(d,p) optimizations (upper profile)

lower profile. Step 1 is the Michael addition of 5-amino-3-methylisoxazole to **3-I1** which takes place via six-membered transition state **TS1**. This step starts with the nucleophilic attack of aromatic amine to the β-C atom of **3-I1**. The activation energy barrier of this step is predicted to be 25.0 kcal/mol. When considering the intrinsic reaction coordinate (IRC) from **RC1** to **3-I2,** this process is slightly endergonic with an energy of 2.2 kcal/mol (Fig. 2).

In step 2, the conversion of **3-I2** to **3-I3** occurs with enol-keto tautomerization. Generally, in triad systems, the keto tautomer is favorable, as the heteroatom prefers π electrons instead of the proton. In parallel to this, we found that keto tautomer **3-I3** was favored over enol tautomer **3-I2** by 11.1 kcal/mol. The calculated Gibbs free energy barrier of **TS2** for enol-keto tautomerization is 15.7 kcal/mol and the reaction is highly exergonic (Fig. 2) as expected.

Step 3 is the cyclization with a new C–C bond formation and can proceed either via O or N as shown in Scheme 5. In the case of cyclization via O, the intramolecular attack of isoxazole carbon (C39) to the carbonyl carbon (C19) of **3-I3** (Fig. 3)

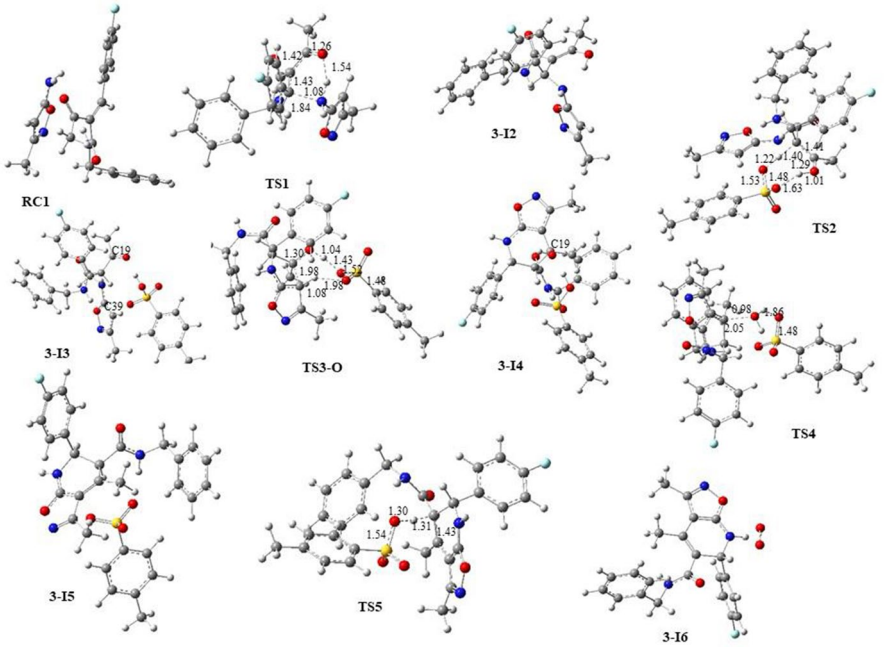

Fig. 3 3-D views of the optimized geometries along the reaction coordinate obtained from M06-2X/6-31G(d,p) method. Distances are given in angstroms. (Color figure online)

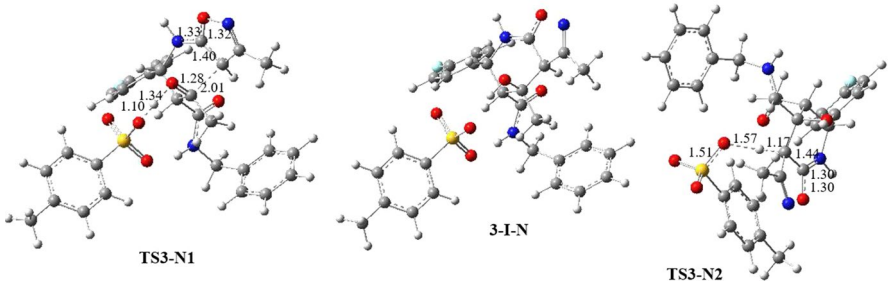

Fig. 4 3-D views of the optimized geometries belonging to "cyclization via N path" obtained from M06-2X/6-31+G(d,p) method. Distances are given in angstroms. (Color figure online)

is triggered by the lone pair electrons of isoxazole oxygen affording the transition state **TS3-O**. However, the assumed intermediate **3-I-O** could not be obtained during the geometry optimizations owing to its unstable character with a positive charge on oxygen. Optimizations after the intrinsic reaction coordinate calculations directly gave rise to **3-I4** with activation energy of 18.5 kcal/mol relative to RC1 (Fig. 2). On the other hand, the intrinsic activation energy of this step from **3-I3** to **3-I4** (27.4 kcal/mol) is noticeably higher, implying that it is the rate-limiting step. According to calculated electronic charges, C39 (− 0.52) is greatly nucleophilic while C19 (0.44) is electrophilic, confirming the proposed attack. Moreover, this

attack generates a stable six-membered ring structure, the precursor of the stable product **4a** which was experimentally observed to be the main product. As a result, the reaction is exergonic by 8.2 kcal/mol. It is important to note that abstraction of the isoxazole proton by *p*-toluenesulfonic acid also facilitates the direct formation of **3-I4**.

The alternative path of step 3 is the cyclization via N where the attack of isoxazole carbon to the carbonyl carbon of **3-I3** is triggered by the lone pair electrons of amine nitrogen giving rise to intermediate **3-I-N** passing through **TS3-N1**. Then, hydrogen abstraction by *p*-toluenesulfonic acid results in the formation of intermediate **3-I4** via **TS3-N2**. The activation energies of these two steps (**TS3-N1** and **TS3-N2**) are relatively smaller (15.1 and 4.9 kcal/mol with respect to **RC1**, respectively) and both steps are exergonic. Moreover, starting from **TS1** (with 24.2 kcal/mol activation energy), the energy profile of this mechanism is always downhill, verifying that it is a feasible mechanism. The intrinsic activation barrier of cyclization via the **TS3-N1** step is 20.7 kcal/mol which is remarkably smaller than the one for cyclization via **TS3-O** (27.4 kcal/mol), revealing that cyclization via the N path is the kinetically preferred mechanism.

The last two steps (steps 4 and 5) are also common steps for both cyclization paths. Because of the extremely smaller energies of these steps relative to **RC1**, the geometry optimizations of the structures from **TS4** to **3-I6** were not repeated with M06-2X/6-31(d,p). Step 4 is an acid-catalyzed dehydration of the OH group at C19 of intermediate **3-I4**. The next step (**TS5**) is the proton abstraction at C24 of intermediate **3-I5**. Figure 2 shows that, due to the highly exergonic feature of the previous steps, both **TS4** and **TS5** have lower energies with respect to **RC1** (− 3.8 kcal/mol and − 1.3 kcal/mol, respectively). Intrinsic energy barriers for step 4 and step 5 are notably small, 13.3 kcal/mol and 10.3 kcal/mol, respectively. The overall Gibbs free energy difference between the first **RC1** and **3-I6** is − 9.7 kcal/mol and demonstrates a quite exergonic process (Fig. 2). Although intermediate **3-I4** appears to be the minimum energy point in this reaction profile, the reaction does not terminate in **3-I4**, but proceeds via **TS4**, **TS5** and end with aromatization via air oxygen. Since the energy barriers of **TS4** and **TS5** are noticeably small and lead to stable products as well, it is reasonable to assume that, under the reaction conditions (RT and long reaction time), a substantial amount of molecules will transform to **3-I6**. Indeed, the extremely grater stability of the final aromatized product **4a** (predicted to be about − 80 kcal/mol) is the driving force of the reaction.

We further performed aromaticity calculations in order to explain why cyclization products of 2-aminoquinoline (benzo[*b*][1,8]naphthyridine-3-carboxamides **6a–c**) formed without aromatization, contrary to isoxazolopyridine in **4a**. We calculated the aromaticity of the pyridine fragment of isoxazolopyridine in **4a** as well as in the aromatized analog of **6a** (Fig. 5) employing the nucleus-independent chemical shifts (NICS) method [13]. NICS values were computed at the ring center [NICS(0)] and 1 Å above the ring [NICS(1)]. It is well-known that significantly negative NICS values indicate the diatropic ring currents confirming the aromatic character of the molecule, while the positive NICS values indicate the paratropic ring currents (antiaromaticity) and small values represent nonaromaticity [14]. It is apparent from Fig. 5 that the pyridine fragment of benzonaphthyridine exhibits considerably smaller

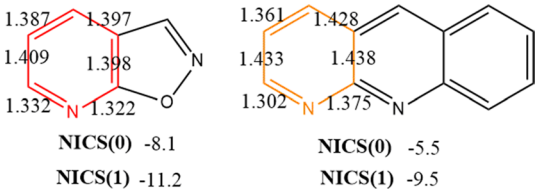

Fig. 5 Calculated bond lengths (Å) and the aromaticity values (ppm) at the ring center [NICS(0)] and 1.0 Å above the ring [NICS(1)] for the pyridine fragments in isoxazolopyridine (red) and in benzonaphthyridine (yellow). (Color figure online)

negative NICS values than that of isoxazolopyridine revealing its weaker aromatic character. Besides, the calculated bond lengths in benzonaphthyridine denote significant bond length alternation [14] confirming the substantial decrease in aromaticity relative to isoxazolopyridine. Thus, the formation of the unaromatized products **6a–c** can be attributed to the insufficient driving force for the aromatization.

Conclusion

In this study, the new isoxazole and naphthyridine derivatives of carboxamides have been synthesized. In the literature, there exists a wide variety of one-pot reactions giving rise to heterocyclic compounds. For similar multi-component, one-pot reactions, several mechanistic pathways can be proposed. However, it is evident from our computational study that the mechanism we propose in Scheme 5 is a plausible one, cyclization via N being more feasible than cyclization via O. The highest energy step of the cyclization via the N mechanism is the first step which exhibits 24.2 kcal/mol of Gibbs activation energy and can be exceeded under the reaction conditions. Moreover, the reaction is downhill and remarkably exergonic which is supposed to be the driving force of this one-pot reaction.

We propose the same mechanism up to step 3 for the reaction with 2-aminoquinoline (Scheme 3) because intermediate **3-I3** corresponds to the compounds **5a–c** when 2-aminoquinoline is used instead of isoxazole. Interestingly, the reaction with 2-aminoquinoline under the same conditions yields **5a–c** without undergoing cyclization. The facile ring closure observed in case of isoxazole can be ascribed to the fact that π-electron density at C–C bond of isoxazole ring is much more accessible for the cyclization when compared to the corresponding bond of 2-aminoquinoline which suffers from annelation of the fused benzene ring.

Isoxazole and naphthyridine derivatives are important compounds in drug discovery because they are expected to show high biological activities. As a matter of fact, anti-cancer (HeLa and pancreas) activity studies of **4a, b** and **4c** were performed as an interdisciplinary study. Compound **4c** is currently being further evaluated. In addition, due to their good UV absorptions, these compounds can be used for further studies in that area.

Experimental

General

Unless otherwise noted, all reagents and solvents were obtained commercially and used without further purification. The solvents were dried by standard procedures. All melting points are uncorrected and were determined on a Gallenkamp digital thermometer. IR spectra were obtained with a Perkin Elmer FT-IR system and are reported in the terms of frequency of absorption (cm^{-1}). ^{1}H and ^{13}C NMR spectra were recorded on a Bruker Avance III-500 MHz NMR spectrometer with TMS as an internal standard. Chemical shifts are reported in parts per million (ppm). Mass spectra were measured either on an Agilent 6890 N/5973 GC/IMSD system or an Agilent 6460 Triple Quad LC/MS system. High-resolution mass spectra were acquired in the positive ion mode using a Agilent G6530B TOF/QTOF mass spectrometer.

General procedures for **4a–d** and **5a–c**. A solution of **3** (0.191 g, 1 mmol) was stirred in 5 mL of dry CH_2Cl_2 for 5 min. Then, the aldehyde (1 mmol), the amine (1 mmol) and *p*-TsOH.H_2O (0.019 g, 0.1 mmol) were added respectively. The reaction mixture was allowed to stir until a precipitate appeared. After completion of the reaction, as indicated by TLC, the reaction mixture was filtered and the residue was washed with methanol and then with ethanol and dried in vacuo.

Procedure for the synthesis of compounds **6a–c**. A solution of **5a** (0.044 g, 0.011 mmol) was stirred in 5 mL of dry CH_3CN for 5 min at 82 °C. Then iodine (8.316 mg, 0.033 mmol) was added to the refluxing mixture and stirred 2 days. After completion of the reaction, as indicated by TLC, CH_3CN was evaporated. The crude material was extracted with a solution of sodium thiosulfate and AcOEt. The organic layer was dried over $MgSO_4$, filtered and concentrated. The residue was purified by column chromatography (5:1 AcOEt/*n*-hexane) to give **6a**.

N-Benzyl-6-(4-fluorophenyl)-3,4-dimethylisoxazolo[5,4-*b*]pyridine-5-carboxamide (4a)

Colorless solid; yield = 45%; mp. 222–224 °C; $R_f = 0.60$ (2:1, ethyl acetate/*n*-hexane); FTIR (ATR): $\nu = 3315$ (N–H), 3060, 3048, 2962, 2920, 2841, 1643 (C=O), 1587, 1581, 1453, 1429, 1358, 1152, 837, 729, 697 cm^{-1}; ^{1}H NMR (500 MHz, DMSO-d_6): $\delta = 1.87$ (*s*, 3H, CH_3), 2.72 (*s*, 3H, CH_3), 4.21 (*d*, $J = 6.25$ Hz, 2H, CH_2), 6.77–6.79 (*m*, 2H, ArH), 7.04–7.12 (*m*, 5H, ArH), 7.34–7.38 (*m*, 2H, ArH), 7.77 (brs, 1H, NH) ppm; ^{13}C NMR (125 MHz, DMSO-d_6): $\delta = 22.5$ (CH_3), 33.0 (CH_3), 53.5 (CH_2), 125.7 (CAr), 125.9 (CAr), 137.5 (2xCAr), 138.1 (2xCAr), 138.9 (CAr), 142.1 (2xCAr), 142.2 (CAr), 149.3 (2xCq), 154.5 (Cq), 167.6 [Cq, *d*, $J_{CF} = 279$ Hz)], 166.1 (2xCq), 177.2 (C=O) ppm; LCMS (ESI-QTOF) *m/z*: calcd. for $C_{22}H_{18}FN_3O_2$ 375.1379; found 376.1453 $[M+H]^+$.

N-Benzyl-6-(4-chlorophenyl)-3,4-dimethylisoxazolo[5,4-*b*]pyridine-5-carboxamide (**4b**)

Colorless solid; yield = 70%; mp. 251–253 °C; R_f = 0.69 (2:1, ethyl acetate/*n*-hexane); FTIR (ATR): ν = 3263 (N–H), 3086, 3060, 2993, 2971, 2926, 1631 (C=O), 1604, 1581, 1554, 1492, 1453,1392, 1083, 829, 714, 691 cm^{-1}; ^{1}H NMR (400 MHz, DMSO-d_6): δ = 1.97 (*s*, 3H, CH_3), 2.58 (*s*, 3H, CH_3), 4.24 (*d*, *J* = 5.99 Hz, 2H, CH_2), 6.76–6.78 (*m*, 2H, ArH), 7.17–7.20 (*m*, 3H, ArH), 7.41 (*d*, *J* = 8.59 Hz, 2H, ArH), 7.51 (*d*, *J* = 8.59 Hz, 2H, ArH), 8.88 (brs, 1H, NH) ppm; ^{13}C NMR (100 MHz, DMSO-d_6): δ = 12.7 (CH_3), 23.1 (CH_3), 42.6 (CH_2), 109.2 (Cq), 127.1 (2xCAr), 127.3 (2xCAr), 128.4 (CAr), 128.6 (2xCAr), 130.4 (Cq), 131.3 (2xCAr), 132.3 (Cq), 134.6 (Cq), 138.8 (Cq), 143.7 (Cq), 156.3 (Cq), 158.0 (Cq), 166.5 (Cq), 168.4 (C=O) ppm; LCMS (ESI-QTOF) *m/z*: calcd. for $C_{22}H_{18}ClN_3O_2$ 391.1088; found 392.1159 $[M+H]^+$.

N-Benzyl-6-(4-nitrophenyl)-3,4-dimethylisoxazolo[5,4-*b*]pyridine-5-carboxamide (**4c**)

Colorless solid; yield = 72%; mp. 272–274 °C; R_f = 0.64 (2:1, ethyl acetate/*n*-hexane); FTIR (ATR): ν = 3261 (N–H), 3082, 3020, 2922, 1633 (C=O), 1601, 1579, 1556, 1518, 1494, 1453,1390, 1346, 1132, 846, 716, 686 cm^{-1}; ^{1}H NMR (500 MHz, $CDCl_3$): δ = 2.04 (*s*, 3H, CH_3), 2.74 (*s*, 3H, CH_3), 4.37 (*d*, *J* = 5.69 Hz, 2H, CH_2), 5.29 (*s*, 1H, CH), 5.81 (brs, 1H, NH), 6.83 (dd, *J* = 2.20; 7.88 Hz, 2H, ArH), 7.23–7.25 (*m*, 3H, ArH), 7.30 (*d*, *J* = 8.51 Hz, 2H, ArH), 7.41 (*d*, *J* = 8.51 Hz, 2H, ArH), 7.77 (brs, 1H, NH) ppm; ^{13}C NMR (125 MHz, DMSO-d_6): δ = 12.1 (CH_3), 22.6 (CH_3), 42.3 (CH_2), 67.1 (CH), 122.9 (CAr), 126.6 (CAr), 127.3 (2xCAr), 127.8 (2xCAr), 129.3 (Cq), 129.4 (CAr), 129.6 (Cq), 130.5 (2xCAr), 138.3 (Cq), 142.3 (Cq), 155.7 (2xCq), 157.7 (2xCq), 165.6 (C=O) ppm; LCMS (ESI-QTOF) *m/z*: calcd. for $C_{22}H_{18}N_4O_4$ 402.1328; found 403.1400 $[M+H]^+$.

N-Benzyl-6-(4-cyanophenyl)-3,4-dimethylisoxazolo[5,4-*b*]pyridine-5-carboxamide (**4d**)

Yellow solid; yield = 37%; mp. 231–233 °C; R_f = 0.61 (2:1, ethyl acetate/*n*-hexane); FTIR (ATR): ν = 3265 (N–H), 3088, 3063, 3024, 2972, 2927, 2873, 2227, 1630 (C=O), 1594, 1583, 1494, 1430, 1391, 1173, 879, 732, 696 cm^{-1}; ^{1}H NMR (500 MHz, DMSO-d_6): δ = 1.95 (*s*, 3H, CH_3), 2.62 (*s*, 3H, CH_3), 4.24 (brd, *J* = 4.41 Hz, 2H, CH_2), 6.81 (*d*, *J* = 6.94 Hz, 2H, ArH), 7.17–7.21 (*m*, 3H, ArH), 7.59 (*d*, *J* = 7.88 Hz, 2H, ArH), 7.89 (*d*, *J* = 7.88 Hz, 2H, ArH), 8.92 (brs, 1H, NH) ppm; ^{13}C NMR (125 MHz, DMSO-d_6): δ = 12.0 (CH_3), 22.6 (CH_3), 42.3 (CH_2), 109.3 (Cq), 112.0 (Cq), 118.4 (2xCq), 126.7 (CAr), 127.1 (2xCAr), 128.0 (2xCAr), 129.6 (Cq), 130.0 (2xCAr), 131.8 (CAr), 137.7 (CAr), 138.3 (Cq), 142.6 (Cq), 155.7 (Cq), 157.7 (Cq), 165.7 (Cq), 167.9 (C=O) ppm; LCMS (ESI-QTOF) *m/z*: calcd. for $C_{23}H_{18}N_4O_2$ 382.1417; found 383.1486 $[M+H]^+$.

N-Benzyl-2-((4-fluorophenyl)(quinolin-2-ylamino)methyl)-3-oxobutanamide (**5a/5a′**, diasteromeric mixture)

Yellow solid; yield = 42%; mp. 139–141 °C; R_f = 0.65 (2:1, ethyl acetate/*n*-hexane); FTIR (ATR): ν = 3378, 3277 (N–H), 3082, 3047, 2993, 2856, 1708 (C=O), 1645, 1617, 1525, 1455, 1443, 1396, 1157, 816, 749, 697 cm^{-1}; ^1H NMR (500 MHz, DMSO-d_6): δ = 2.24 (*s*, 3H, CH_3), 3.92 (dd, *J* = 4.41; 15.4 Hz, 1H, CH_2), 4.00 (*d*, *J* = 11.98 Hz, 1H, CH), 4.18 (*d*, *J* = 11.35 Hz, 1H, CH), 4.33 (dd, *J* = 7.25; 15.4 Hz, 1H, CH_2), 6.04 (brs, 1H, NH), 6.67 (*d*, *J* = 6.93 Hz, 1H, ArH), 6.74 (*d*, *J* = 9.14 Hz, 1H, ArH), 7.08–7.19 (*m*, 6H, ArH), 7.45–7.49 (*m*, 1H, ArH), 7.51–7.56 (*m*, 3H, ArH), 7.60 (*d*, *J* = 7.25 Hz, 1H, ArH), 7.73 (*d*, *J* = 9.45 Hz, 1H, ArH), 7.83 (*d*, *J* = 8.82 Hz, 1H, ArH), 8.76 (brs, 1H, NH) ppm; ^{13}C NMR (125 MHz, DMSO-d_6, both diastereomers): δ = 27.9 (CH_3), 41.9 (CH_2), 52.8 (CH), 67.0 (CH), 114.5 (CAr), 114.7 (CAr), 121.6 (CAr), 123.0 (Cq), 125.9 (CAr), 126.6 (2xCAr), 126.9 (CAr), 127.4 (CAr), 127.9 (2xCAr), 128.1 (CAr), 129.1 (CAr), 129.8 (CAr), 129.9 (CAr), 136.5 (CAr), 137.6 (Cq), 137.7 (Cq), 138.6 (Cq), 147.4 (Cq), 155.8 (Cq), 161.3 (Cq, J_{CF} = 248 Hz), 165.6 (amide C=O), 202.8 (C=O) ppm; LCMS (ESI-QTOF) *m/z*: calcd. for $C_{27}H_{24}FN_3O_2$ 441.1868; found 442.1935 $[M+H]^+$.

N-Benzyl-2-((4-chlorophenyl)(quinolin-2-ylamino)methyl)-3-oxobutanamide (**5b**)

Colorless solid; yield = 65%; mp. 142–146 °C; R_f = 0.58 (2:1, ethyl acetate/*n*-hexane); FTIR (ATR): ν = 3375, 3270 (N–H), 3077, 3072, 2997, 2948, 2913, 1711 (C=O), 1644, 1618, 1609, 1563, 1489, 1479,1394, 1163, 817, 747, 698 cm^{-1}; ^1H NMR (500 MHz, $CDCl_3$): δ = 2.09 (*s*, 3H, CH_3), 3.98 (dd, *J* = 8.51; 20.8 Hz, 2H, CH_2), 4.18 (*d*, *J* = 5.67 Hz, 1H, CH), 4.26 (*d*, *J* = 5.67 Hz, 1H, CH), 6.00 (brs, 1H, NH), 6.58 (*d*, *J* = 8.82 Hz, 1H, ArH), 6.88 (*d*, *J* = 6.93 Hz, 2H, ArH), 6.98–7.09 (*m*, 3H, ArH), 7.15–7.21 (*m*, 3H, ArH), 7.32 (*d*, *J* = 8.51 Hz, 2H, ArH), 7.42–7.55 (*m*, 3H, ArH), 7.71 (*d*, *J* = 8.82 Hz, 1H, ArH), 9.06 (*s*, 1H, NH) ppm; ^{13}C NMR (125 MHz, DMSO-d_6): δ = 31.3 (CH_3), 46.8 (CH_2), 58.1 (CH), 72.3 (CH), 117.1 (CAr), 126.3 (CAr), 126.4 (Cq), 128.0 (2xCAr), 130.6 (CAr), 130.8 (CAr), 131.2 (CAr), 131.4 (CAr), 131.8 (CAr), 132.4 (2xCAr), 133.4 (CAr), 134.0 (CAr), 134.2 (CAr), 136.4 (CAr), 141.1 (Cq), 143.1 (Cq), 145.0 (Cq), 152.3 (Cq), 160.2 (Cq), 170.3 (C=O), 189.6 (C=O) ppm; LCMS (ESI-QTOF) *m/z*: calcd. for $C_{27}H_{24}ClN_3O_2$ 457.1543; found 458.1604 $[M+H]^+$.

N-Benzyl-2-((4-cyanophenyl)(quinolin-2-ylamino)methyl)-3-oxobutanamide (**5c**)

Colorless solid; yield = 47%; mp. 178–181 °C; R_f = 0.60 (2:1, ethyl acetate/*n*-hexane); FTIR (ATR): ν = 3386, 3261 (N–H), 3064, 1717 (C=O), 1650, 1619, 1530, 1482, 1401, 1357, 1164, 823, 757, 697 cm^{-1}; ^1H NMR (500 MHz, DMSO-d_6): δ = 2.25 (*s*, 3H, CH_3), 3.90 (dd, *J* = 4.41, 15.44 Hz, 1H, CH_2), 4.06 (*d*, *J* = 11.66 Hz, 1H, CH), 4.23 (*d*, *J* = 7.56 Hz, 1H, CH), 4.31 (dd, *J* = 6.93, 15.13 Hz, 1H, CH_2), 6.03 (brs, 1H, NH), 6.66 (*d*, *J* = 6.93 Hz, 1H, ArH), 6.75 (*d*, *J* = 8.82 Hz, 1H, ArH), 7.01 (dd, *J* = 2.20; 5.99 Hz, 1H, ArH), 7.12–7.19 (*m*, 4H, ArH), 7.46 (ddd, *J* = 1.57; 8.19; 15.1 Hz, 1H, ArH), 7.53 (*d*, *J* = 8.19 Hz, 1H, ArH), 7.59 (*d*, *J* = 8.19 Hz, 1H, ArH),

7.66–7.70 (*m*, 3H, ArH), 7.83 (*t*, $J=8.19$ Hz, 2H, ArH), 8.80 (brs, 1H, NH) ppm; ^{13}C NMR (125 MHz, DMSO-d_6): $\delta=28.1$ (CH_3), 41.8 (CH_2), 53.3 (CH), 66.1 (CH), 109.7 (Cq), 118.8 (Cq), 121.7 (CAr), 123.1 (Cq), 125.7 (CAr), 125.8 (CAr), 126.6 (2xCAr), 126.8 (Ar), 127.4 (CAr), 127.9 (CAr), 128.0 (CAr), 128.3 (CAr), 129.0 (CAr), 129.1 (CAr), 131.8 (CAr), 131.9 (CAr), 136.6 (CAr), 138.5 (Cq), 147.2 (Cq), 147.6 (Cq), 155.6 (Cq), 165.1 (C=O), 202.1 (C=O) ppm; LCMS (ESI-QTOF) *m/z*: calcd. for $C_{28}H_{24}N_4O_2$ 446.1744; found 447.1815 $[M+H]^+$.

N-Benzyl-2-(4-fluorophenyl)-4-methyl-1,2-dihydrobenzo[*b*][1,8] naphthyridine-3-carboxamide (**6a/6a′**, cis–trans amide isomers)

Yellow oil; yield = 36%; $R_f=0.32$ (5:1, ethyl acetate/*n*-hexane); FTIR (ATR): $\nu=3356$ (N–H), 3068, 3044, 2962, 2923, 2851, 1704 (C=O), 1673, 1605, 1579, 1453, 1410, 1353, 1156, 839, 748, 698 cm^{-1}; ^{1}H NMR (500 MHz, $CDCl_3$): $\delta=2.43$ (*s*, 3H, CH_3), 3.70 (dd, $J=5.35$; 14.50 Hz, 1H, CH_2), 4.07 (dd, $J=5.35$; 14.50 Hz, 1H, CH_2), 5.41 (*s*, 1H, CH), 6.27 (*d*, $J=8.19$ Hz, 1H, ArH), 6.74 (*d*, $J=9.77$ Hz, 1H, ArH), 6.90–6.92 (*m*, 2H, ArH), 6.94–6.97 (*m*, 2H, ArH), 6.98–7.03 (*m*, 2H, ArH), 7.22–7.25 (*m*, 4H, ArH and NH), 7.37–7.40 (*m*, 3H, ArH), 7.99 (brs, 1H, NH) ppm; ^{13}C NMR (125 MHz, $CDCl_3$, both cis–trans isomers): $\delta=26.0$, 29.7 (CH_3), 43.7, 44.1 (CH_2), 79.2, 82.0 (CH), 111.89, 111.95 (CAr), 114.98, 115.1 (CAr), 115.3, 115.5(CAr), 116.9, 117.1 (CAr), 121.6, 121.7 (CAr), 121.5, 121.6 (Cq), 127.5, 127.8, (CAr), 127.9, 128.1 (CAr), 128.6, 128.9.0 (CAr), 129.16, 129.18 (CAr), 129.7, 129.8 (CAr), 130.4, 130.5 (CAr), 130.7, 130.8 (CAr), 133.1, 133.3 (Cq), 137.3, 137.9 (Cq), 138.1, 138.4 (Cq), 138.3 (CAr), 157.9, 158.5 (Cq), 162.7 (Cq, $J_{CF}=246$ Hz), 162.9 (Cq, $J_{CF}=246$ Hz) 168.1 (C=O amide), 209.3 (C=O) ppm; LCMS (ESI-QTOF) *m/z*: calcd. for $C_{27}H_{22}FN_3O$ 423.1768; found 423.1763 $[M]^+$.

N-Benzyl-2-(4-chlorophenyl)-4-methyl-1,2-dihydrobenzo[*b*][1,8] naphthyridine-3-carboxamide (**6b**)

Yellow oil; yield = 34%; $R_f=0.46$ (5:1, ethyl acetate/*n*-hexane); FTIR (ATR): $\nu=3335$ (N–H), 3062, 3030, 2956, 2923, 2851, 1706 (C=O), 1640, 1614, 1581, 1453, 1410, 1354, 1139, 811, 748, 698 cm^{-1}; ^{1}H NMR (500 MHz, $CDCl_3$): $\delta=2.43$ (*s*, 3H, CH_3), 3.73 (dd, $J=5.35$; 14.50 Hz, 1H, CH_2), 4.05 (dd, $J=5.35$; 14.50 Hz, 1H, CH_2), 5.43 (*s*, 1H, CH), 6.31 (*d*, $J=8.19$ Hz, 1H, ArH), 6.83 (*d*, $J=9.45$ Hz, 1H, ArH), 6.89–6.90 (*m*, 2H, ArH), 7.05 (*d*, $J=7.25$ Hz, 1H, ArH), 7.17–7.29 (*m*, 5H, ArH and NH), 7.36–7.38 (*m*, 2H, ArH), 7.42–7.45 (*m*, 2H, ArH), 7.47 (*m*, 1H, ArH), 7.97 (brs, 1H, NH) ppm; ^{13}C NMR (125 MHz, $CDCl_3$): $\delta=29.7$ (CH_3), 43.8 (CH_2), 78.0 (CH), 112.0 (CAr), 121.6 (Cq), 121.7 (Cq), 121.9 (CAr), 127.5 (CAr), 127.8 (CAr), 128.0 (CAr), 128.3 (CAr), 128.5 (CAr), 128.7 (CAr), 128.8 (CAr), 129.2 (CAr), 129.9 (CAr), 130.9 (CAr), 131.0 (CAr), 134.6 (Cq), 135.5 (Cq), 137.0 (Cq), 137.5 (Cq), 138.0 (Cq), 138.8 (CAr), 158.6 (Cq), 162.6 (Cq), 167.7 (C=O) ppm; LCMS (ESI-QTOF) *m/z*: calcd. for $C_{27}H_{22}ClN_3O$ 437.1275; found 438.1350 $[M+H]^+$.

N-Benzyl-2-(4-cyanophenyl)-4-methyl-1,2-dihydrobenzo[*b*][1,8] naphthyridine-3-carboxamide (6c)

Yellow oil; yield = 30%; R_f = 0.32 (3:1, ethyl acetate/*n*-hexane); FTIR (ATR): ν = 3343 (N–H), 3063, 3032, 2955, 2921, 2850, 2226, 1705 (C=O), 1640, 1609, 1580, 1453, 1411, 1354, 1138, 841, 748, 698 cm^{-1}; ^{1}H NMR (500 MHz, $CDCl_3$): δ = 2.44 (*s*, 3H, CH_3), 3.78 (dd, *J* = 5.86; 14.67 Hz, 1H, CH_2), 3.99 (dd, *J* = 5.86; 14.67 Hz, 1H, CH_2), 5.43 (*s*, 1H, CH), 6.28 (*d*, *J* = 7.82 Hz, 1H, ArH), 6.75 (*d*, *J* = 9.29 Hz, 1H, ArH), 6.90 (dd, *J* = 2.44; 7.82 Hz, 2H, ArH), 7.04 (*t*, *J* = 7.82 Hz, 1H, ArH), 7.27–7.29 (*m*, 3H, ArH ve NH), 7.37 (*t*, *J* = 7.82 Hz, 2H, ArH), 7.42 (*d*, *J* = 9.29 Hz, 2H, ArH), 7.47 (*d*, *J* = 8.31 Hz, 2H, ArH), 7.57 (*d*, *J* = 8.31 Hz, 1H, ArH), 8.12 (brs, 1H, NH) ppm; ^{13}C NMR (125 MHz, $CDCl_3$): δ = 26.9 (CH_3), 43.6 (CH_2), 78.8 (CH), 111.7 (CAr), 112.2 (Cq), 116.6 (CAr), 118.7 (2xCq), 121.5 (2xCq), 121.7 (CAr), 127.7 (CAr), 127.9 (CAr), 128.1 (CAr), 128.6 (CAr), 128.7 (CAr), 128.9 (CAr), 129.3 (CAr), 130.8 (CAr), 131.6 (CAr), 132.1 (CAr), 136.9 (Cq), 138.0 (Cq), 138.4 (Cq), 138.6 (CAr), 142.5 (Cq), 153.9 (Cq), 162.6 (C=O) ppm; LCMS (ESI-QTOF) *m/z*: calcd. for $C_{28}H_{22}N_4O$ 434.2118; found 452.2457 $[M+NH_4]^+$.

Theoretical calculations

Geometrical parameters of reactants, intermediates (I), transition states (TS) and products were fully optimized in the gas phase with the density functional theory with the M06-2X [15] functional using the 6-31G(d,p) and 6-31+G(d,p) basis sets implemented in Gaussian 09 [16] for cyclization via O and cyclization via N paths, respectively. M06-2X is known to show good performance in accounting for the weak hydrophobic forces' so-called dispersion effect. Recently, we have successfully applied the same method to different reaction mechanisms [17–19]. All stationary points were characterized by frequency calculations with only one imaginary frequency for the transition states. Intrinsic reaction coordinate (IRC) [20–22] was also searched to verify each step of the mechanism. To take into account the solvent effect, single-point energy calculations with the polarizable continuum model (PCM) [23, 24] were carried out at the M06-2X/6-311++G(d,p) level with dichloromethane (CH_2Cl_2) as the solvent, since this solvent was used in the experimental study. NICS values were calculated using the gauge-independent atomic orbital (GIAO) theory [25] at the M06-2X/6-311++G(d,p)//M06-2X/6-31+G(d,p) level.

Acknowledgements N. Ocal gratefully acknowledges financial support of this work by the Scientific and Technological Research Council of Turkey (TUBITAK, project no. 112T880). I. Erden acknowledges financial support of this work by funds from the National Institutes of Health (grant no. SC1GM082340). The numerical calculations reported in this paper were partially performed at TUBITAK ULAKBIM, High Performance and Grid Computing Center (TRUBA resources).

References

1. A. Shaabani, M. Seyyedhamzeh, A. Maleki, M. Behnam, Tetrahedron Lett. **50**, 6355 (2009)
2. V.P. Litvinov, S.V. Roman, V.D. Dyachenko, Russ. Chem. Rev. **69**, 220 (2000)
3. M.H. Sherlock, J.J. Kaminsky, W.C. Tom, J.F. Lee, S.C. Wong, R.W. Bryant, A.T. McPhail, J. Med. Chem. **31**, 2108 (1988)
4. B.A. Johns, J.G. Weatherhead, S.H. Allen, J.B. Thompson, E.P. Garvey, S.A. Foster, J.L. Jeffrey, W.H. Miller, Bioorg. Med. Chem. Lett. **19**, 1802 (2009)
5. B.A. Johns, J.G. Weatherhead, S.H. Allen, J.B. Thompson, E.P. Garvey, S.A. Foster, J.L. Jeffrey, W.H. Miller, Bioorg. Med. Chem. Lett. **19**, 1807 (2009)
6. K.A. Kumar, P. Jayaroopa, J. Pharm. Chem. Biol. Sci. **3**(2), 294 (2013)
7. P. Nagender, G.M. Reddy, R.N. Kumar, Y. Poornachandra, C.G. Kumar, B. Narsaiah, Bioorg. Med. Chem. Lett. **24**, 2905 (2014)
8. A. Shaabani, M. Seyyedhamzeh, A. Maleki, M. Behnam, F. Rezazadeh, Tetrahedron Lett. **50**, 2911 (2009)
9. S.B. Bharate, T.R. Mahajan, Y.R. Gole, M. Nambiar, T.T. Matan, A. Kulkarni-Almeida, S. Balachandran, H. Junjappa, A. Balakrishnan, R.A. Vishwakarma, Bioorg. Med. Chem. **16**, 7167 (2008)
10. V.V. Tkachenko, E.A. Muravyova, S.V. Shishkina, O.V. Shishkin, S.M. Desenko, V.A. Chebanov Chem, Heterocycl. Compd. **50**, 1166 (2014)
11. N. Ocal, N. Mor, I. Erden, Tetrahedron Lett. **56**, 6468 (2015)
12. X.S. Wang, Q. Li, C.S. Yao, S.J. Tu, Eur. J. Org. Chem. **20**, 3513 (2008)
13. Z. Chen, C.S. Wannere, C. Corminboeuf, R. Puchta, P.V.R. Schleyer, Chem. Rev. **105**, 3842 (2005)
14. S.S. Erdem, G.A. Özpınar, M.T. Saçan, J. Mol. Struct. Theochem **726**, 233 (2005)
15. Y. Zhao, D.G. Truhlar, Theor. Chem. Acc. **120**, 215 (2008)
16. M.J. Frisch, G.W. Trucks, H.B. Schlegel, G.E. Scuseria, M.A. Robb, J.R. Cheeseman, G. Scalmani, V. Barone, G.A. Petersson, H. Nakatsuji, X. Li, M. Caricato, A. Marenich, J. Bloino, B.G. Janesko, R. Gomperts, B. Mennucci, H.P. Hratchian, J.V. Ortiz, A.F. Izmaylov, J.L. Sonnenberg, D. Williams-Young, F. Ding, F. Lipparini, F. Egidi, J. Goings, B. Peng, A. Petrone, T. Henderson, D. Ranasinghe, V.G. Zakrzewski, J. Gao, N. Rega, G. Zheng, W. Liang, M. Hada, M. Ehara, K. Toyota, R. Fukuda, J. Hasegawa, M. Ishida, T. Nakajima, Y. Honda, O. Kitao, H. Nakai, T. Vreven, K. Throssell, J.A. Montgomery Jr., J.E. Peralta, F. Ogliaro, M. Bearpark, J.J. Heyd, E. Brothers, K.N. Kudin, V.N. Staroverov, T. Keith, R. Kobayashi, J. Normand, K. Raghavachari, A. Rendell, J.C. Burant, S.S. Iyengar, J. Tomasi, M. Cossi, J.M. Millam, M. Klene, C. Adamo, R. Cammi, J.W. Ochterski, R.L. Martin, K. Morokuma, O. Farkas, J.B. Foresman, D.J. Fox, Gaussian 09, Revision B.01 (Gaussian Inc., Wallingford, CT, 2010)
17. S.E. Gunal, G.S. Gurses, S.S. Erdem, I. Dogan, Tetrahedron **72**, 2122 (2016)
18. K. Cakir, S.S. Erdem, V.E. Atalay, Org. Biomol. Chem. **14**, 9239 (2016)
19. M.A. Akyüz, S.S. Erdem, J. Neural Transm. **120**, 937 (2013)
20. C. Gonzalez, H.B. Schlegel, J. Chem. Phys. **90**, 2154 (1989)
21. C. Gonzalez, H.B. Schlegel, J. Chem. Phys. **94**, 5523 (1990)
22. K. Fukui, Acc. Chem. Res. **14**, 363 (1981)
23. S. Miertus, E. Scrocco, J. Tomasi, Chem. Phys. **55**, 117 (1981)
24. J. Tomasi, B. Mennucci, R. Cammi, Chem. Rev. **105**, 2999 (2005)
25. K. Wolinski, J.F. Hinton, P. Pulay, J. Am. Chem. Soc. **112**, 8251 (1990)